MSc in Photonics

PHOTONICS**BCN**

Universitat Politècnica de Catalunya (UPC)
Universitat Autònoma de Barcelona (UAB)
Universitat de Barcelona (UB)
Institut de Ciències Fotòniques (ICFO)

http://www.photonicsbcn.eu

Master in Photonics

MASTER THESIS WORK

QUANTUM EFFECTS AND GAP MORPHOLOGY IN THE OPTICAL RESPONSE OF PLASMONIC GAP-NANOANTENNAS

Garikoitz Aguirregabiria Achutegui

Supervised by Dr. Javier Aizpurua (MPC) and Dr. Ruben Esteban (DIPC)

Presented on date 9th September 2013

Registered at

Escola Tècnica Superior d'Enginyeria de Telecomunicació de Barcelona

Quantum effects and gap morphology in the optical response of plasmonic gap-nanoantennas

Garikoitz Aguirregabiria Achutegui

Centro de Física de Materiales, Centro mixto CSIC-UPV/EHU, 20018 Donostia-San Sebastian, Spain

E-mail: garikoitz_aguirregabiria001@ehu.es

Abstract. Optical gap-nanoantennas are basic building blocks to control light at the nanoscale. We study how the morphology of the gap affects the response of the nanoantennas. A classical study shows that in spherical gaps the spectral position of the modes redshifts very strongly as the gap distance is reduced, whereas flat gaps present a saturation of the redshift. Moreover, flat-gap antennas show additional plasmon cavity modes that are not present in the far field, contrary to the spherical gaps where far-field and near-field spectra present the same set of modes. We analyze small gap distances where quantum effects need to be included in the description of the response due to electron tunneling. Using a Quantum Corrected Model, we show how tunneling can strongly modify the response. The near-field enhancement is strongly quenched as a consequence of tunneling and this effect depends strongly on the gap morphology. We also find that the spectral transition between non-touching and the overlapping regime for spherical-gap antennas dramatically changes in comparison with classical simulations.

Keywords: Optical Nanoantennas, Quantum Plasmonics, Quantum Corrected Model

1. Introduction

Metallic surfaces exhibit plasmonic modes which are collective oscillations of the conduction electrons of the metal that can be efficiently excited by electromagnetic (EM) fields at optical frequencies. For finite particles, these plasmonic resonances are characterized by localization of charges at the boundaries of the particle, known as Localized Surface Plasmon Polaritons (LSPPs). Some characteristic effects of such plasmons are the strong confinement and enhancement of the EM fields around the nanoparticle as well as the efficient radiation of light at particular resonance frequencies similar to classical radiofrequency antennas.[1,2] This is the reason why these nanostructures are commonly named as optical nanoantennas.

The frequency-dependent dielectric response of a metal $\varepsilon_m(\omega)$ to the EM field can be described by means of a simple harmonic oscillator model to describe the collective motion of electrons in the so-called Drude model:

$$\varepsilon_m(\omega) = \varepsilon_\infty - \frac{\omega_p^2}{\omega(\omega + i\gamma_p)} \tag{1}$$

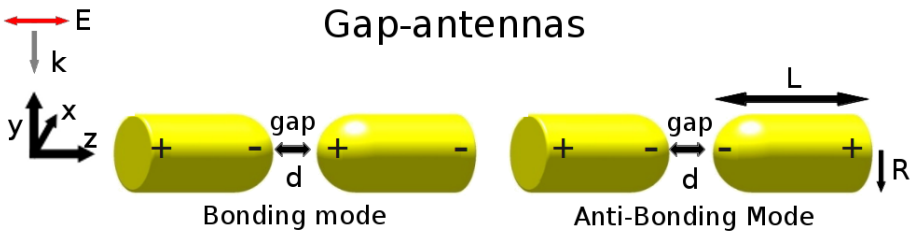

Figure 1. Schematics of the charge distribution of the first order Bonding Mode (left) and Anti-Bonding Mode (right).

where ω_p is the bulk plasma frequency of the metal and γ_p is the damping coefficient. The parameter ε_∞ is related to the dielectric screening of the valence electrons of the ion cores, and the negative part in Eq.(1) is due to the conduction electrons of the material. The value of these parameters is critical to determine the dispersion relation and the absorption of the metal, which is crucial to determine the coupling between the conduction electrons and the EM field. Plasmonic resonances can arise when the real part of the dielectric function takes negative values, i.e. for frequencies smaller than ω_p.

The spectral position of the resonances and the capability of the nanoantenna to absorb, confine and enhance light strongly depends on the constituent material, its size and shape. Depending on the size and shape, the boundary conditions of the fields will change and the surface charges will be distributed in a characteristic manner, therefore different LSPP modes will be supported.

In this thesis we will focus on an additional basic mechanism to control the plasmonic resonances: the Coulomb interaction between surface charges in plasmonic nano-structures. The interaction between nearby nanoantenna arms hybridizes the plasmonic modes of each arm creating bonding modes (BMs) [left antenna in Figure 1] and anti-bonding modes (ABMs) [right antenna in Figure 1] of the coupled antenna system.[3,4] In the BMs, charges of opposite sign pile up at the gap surfaces creating a low energy hybridized plasmon mode that can be excited by optical means while in the ABMs, charges of the same sign pile up at the gap creating higher energy modes that cannot be excited optically. Coupled plasmonic resonances change their energy dramatically with the variations of the gap distance and morphology, thus establishing a powerful ruler to tune the optical response of plasmonic antennas.

Classical electrodynamic computational methods are commonly used to investigate the optical response of plasmonic structures providing good agreement with most experimental measurements.[2,5,6] However, a classical approach based on linear dielectric response theory within Maxwell's equations shows some limitations. In particular, when the gap between objects is reduced to subnanometric distances, the classical theory is not able to describe neither the quantum nature of the non-local interactions between the electrons at the interfaces nor the spill-out of the electron wavefunctions out of the boundaries of the metal.[7–9] Furthermore, at sub-nanometric gap separations, the electronic wavefunctions of both arms overlap and therefore tunneling of electrons

may occur between both bodies of the antenna. As the gap distance is reduced, the probability of quantum tunneling increases and starts to play a fundamental role in determining the optical response of the system. Classical theory is thus not valid to describe antennas with gaps well below 1 nm. To analyze these sub-nanometric gaps, ab-initio quantum mechanical simulations need to be implemented. However, typical nanoantennnas have millions of conducting electrons and full quantum simulations are limited to systems with a few thousands of electrons due to current computational limits. Therefore it is not possible to tackle the optical response of a large and realistic plasmonic system by means of ab-initio calculations. A recently developed method to study the region of sub-nanometric gaps is the Quantum Corrected Model (QCM).[10] This model allows to use a classical electrodynamical approach to calculate the optical response of realistic sized gap-antennas in the regime of sub-nanometric gaps by incorporating quantum tunneling via an effective material that describes the quantum nature of the gap.

In this thesis we analyze how the morphology of the gap affects the response of coupled optical gap-antennas. In particular we will compare the optical response of linear gap-antennas with spherical-gap and flat-gap terminations. We study a range of distances covering from large separations to the overlapping regime. Classical calculations and simulations that include the QCM will be performed in order to study how the consideration of tunneling affects the optical response of each structure for very small gap distances. The dependence of the optical response of an antenna on the fine details of the gap morphology can establish protocols of design in field-enhanced spectroscopy and in optoelectronic devices.

2. Optical gap nanoantennas

We consider optical antennas that consist of two gold nano-rods of length $L = 100$ nm, with a radius of $R = 25$ nm separated by a gap of distance d. The antenna arms show either spherical ends or flat ends at the gap [as sketched in Figure 1]. The far-ends of both antennas are considered to be flat. To avoid unphysically sharp edges a small rounding of radius $r = 2$ nm is considered in the flat areas of the far-ends of both geometries and in the flat-gap. We describe the optical response of the metal by a Drude model where for simplicity we neglect the dielectric screening in Eq.(1) ($\varepsilon_\infty = 1$). We consider a value of $\omega_p = 7.9$ eV and $\gamma_p = 0.09$ eV which correspond to the jellium model of gold (the jellium model is a commonly used framework in many-body physics that describes an electron gas as an homogeneous isotropic electronic density with an ionic core background).

For spherical-gap antennas we find a behavior similar to the intensively studied spherical dimer.[5] We find a very strong redshift of the low energy BM [black dashed line in Figure 2(a)] as well as of other higher-order bonding modes as the gap is reduced towards the touching limit (point at which the arms of the antenna make contact to each other). The near field enhancement [Figure 2(b)] evaluated at the central point of

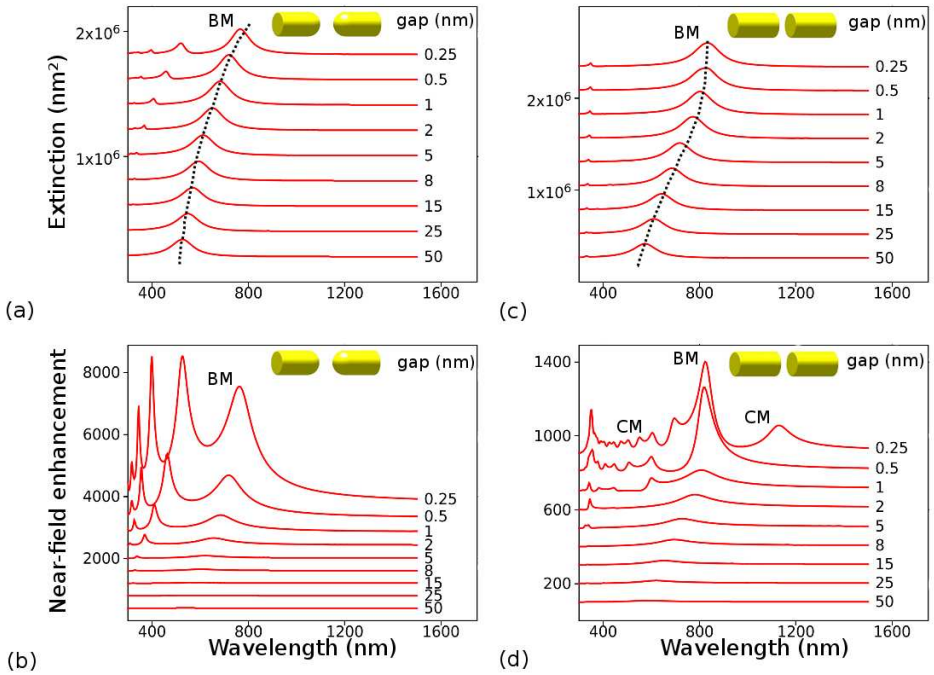

Figure 2. Classical simulations of the response of gap-antennas. (a,c) Extinction cross section and (b,d) local field enhancement $|E/E_0|$ of the (a,b) spherical-gap antenna and (c,d) flat-gap antenna between 50 nm to 0.25 nm. We indicate in the figures the nature of some of the modes (BMs and CMs).

the gap, i.e. the ratio between the near-field and the incoming electric field amplitude $|E/E_0|$, increases very strongly as the gap is reduced because of the pile up of charges at the gap region. The structure of modes can be identified and correlated in both the far-field and the near-field spectrum.

In contrast, flat-gap antennas [Figure 2(c) and 2(d)] show a notably different behavior. As the gap is reduced we find a low energy BM that redshifts for narrowing gaps, similar to the spherical-gap case, but the spectral position saturates when the contact point is approached [black dashed line in Figure 2(c)], and a higher order mode that does not change its spectral position appears in the far-field spectrum. The saturation of the spectral position of the BM can be explained by describing the gap as a capacitor.[11] As the gap distance is diminished the capacitance of the gap, $C_g \propto 1/d$, grows and its impedance thus diminishes, $Z_g \propto 1/C_g$. Therefore, when the gap distance is very small, Z_g is also very small and it behaves like a short-circuit for the fields parallel to the rods axis. In this limiting case, the system behaves as one single $2L$-length rod. For large gap distances, the same modes are found in the near-field but as the distance is reduced, a new set of modes appear [CM in Figure 2(d)]. These modes, redshift very strongly instead of saturating. We identify this new set of modes as Fabry-Perot cavity plasmon modes (CMs).[12–14] Plasmonic cavity modes propagate inside the bounded surface with effective wavelength that has to satisfy the condition $n\lambda_{eff}/2 = D$ (neglecting reflection phase) where D is the characteristic dimension of the cavity and

λ_{eff} is the characteristic wavelength of the excited plasmon. In this case, $D = 2R$ and the plasmon can be associated to the metal-insulator-metal (MIM) structure at the gap. The general trend of the maximum near-field enhancement is to grow as the gap distance is reduced, with particularly strong enhancement when the cavity modes and the far-field modes coincide spectrally. The comparison of the response of both flat-gap and spherical-gap antennas shows that the gap morphology introduces a considerably different optical response in plasmonic nanoantennas.

For gaps well below one nanometer classical simulation methods are not longer valid. To analyze this region we need to introduce quantum effects in our model i.e. in Figure 2, the results for 0.25 nm gap need to be corrected because they do not incorporate the quantum tunneling that is present at those gap distances.

3. Quantum Corrected Model

The Quantum Corrected Model was recently developed to describe the plasmonic response of large metallic gap antennas in close proximity, by incorporating quantum tunneling effects in a classical electrodynamic computational framework.[10,15] The QCM introduces the tunneling current via an effective conducting material placed in the gap that mimics the effect of transport in the quantum tunneling regime. The gap material has different properties depending on the tunneling probability for each gap distance. For non-flat gaps, the distance between the gap surfaces is not constant thus each point at the gap has a characteristic tunneling probability and needs to be described by the corresponding effective dielectric material. We consider several regions in the gap to obtain convergence of the results, as schematically depicted in Figure 3.

Within the QCM, the medium at the gap will be characterized by a Drude-like local dielectric function that will depend on the gap distance at each point of the gap, i.e. $\varepsilon_g(l,\omega)$ where $l = l(x,y)$ with (x,y) the transverse coordinates of the gap (see schematics in Figure 3 for reference):

$$\varepsilon_g(l,\omega) = \varepsilon_{\infty,g}(l) - \frac{\omega_g^2(l)}{\omega(\omega + i\gamma_g(l))} \tag{2}$$

with ω_g the gap plasma frequency and γ_g the gap damping. At contact point, $l = 0$, we recover the dielectric function of gold, therefore we set $\epsilon_{\infty,g} = 1$ and $\omega_g = \omega_p$. Accordingly, the dependence on the distance of the dielectric function is incorporated through the damping coefficient $\gamma_g = \gamma_g(l)$. We can relate γ_g with the tunneling probability by means of the conductivity in the gap. The relationship between the conductivity and the dielectric function is given by

$$\sigma(l,\omega) = -i\frac{\omega}{4\pi}(\varepsilon(l,\omega) - 1) \ . \tag{3}$$

If we now insert Eq.(2) into Eq.(3) and examine the limit of static conductivity, $\omega \to 0$, we find that the damping coefficient can be directly related to the static

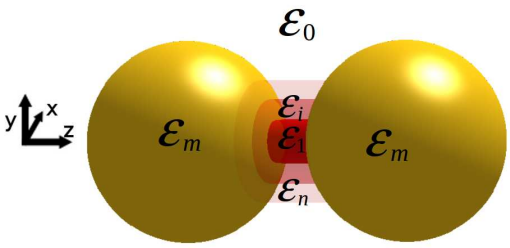

Figure 3. Geometry used to implement the QCM for a spherical dimer of two gold spherical particles with dielectric permitivity ε_m surrounded by vacuum with ε_0. In the gap, several effective media are distributed with permitivities $\varepsilon_1, \ldots, \varepsilon_i, \ldots, \varepsilon_n$.

conductivity $\sigma_0(l) = \sigma(l, \omega \to 0)$, resulting in the expression for the tunneling damping γ_g as:

$$\gamma_g(l) = \frac{\omega_p^2}{4\pi\sigma_0(l)} \quad . \tag{4}$$

Eqs.(3,4) are in atomic units. We obtain the static conductivity from a quantum mechanical calculation for each gap distance $l(x, y)$. The quantum mechanical calculations are made for a simpler systems composed by two gold flat surfaces where the tunneling probability between them, due to the interaction with the static electric field, is calculated via density functional theory (DFT) (Calculations provided by Andrei Borisov's group at Orsay, France). Using Eq.(4) we can obtain γ_g and from there we establish the inhomogeneous $\varepsilon_g(l, \omega)$ at the gap.

DFT calculations show that the tunneling probability between two jellium-like surfaces of gold starts to be significant at separation distances between $0.3 - 0.4$ nm.[10] Therefore, in order to include tunneling for all gap distances where it is relevant we use the QCM for gap distances $d < 0.5$ nm. For the spherical-gap antenna we distribute 5 different effective materials in the gap region where $l(x, y) < 0.5$ nm. To calculate the local dielectric function at the gap we use the averaged gap distance at each section. For flat-gap antennas we insert one medium in the gap covering the whole flat area and neglect the possible tunneling that would take place in the proximity of the rounded corners.

4. Results

In Figures 4 and 5 we have plotted the results of the extinction cross section (Figure 4) and the near-field enhancement (Figure 5) as a function of gap distance and wavelength. Each figure shows the results for the spherical-gap antenna [(a),(c)] and the flat-gap antenna [(c),(d)] using the classical theory [(a),(c)] and the Quantum Corrected Model [(b),(d)]. In section 2 we already analyzed the classical response of the antennas as a function of the gap distance for large gaps, and we now focus on the study of very small gaps and the overlapping regime where the quantum tunneling is crucial in determining the response of the system.

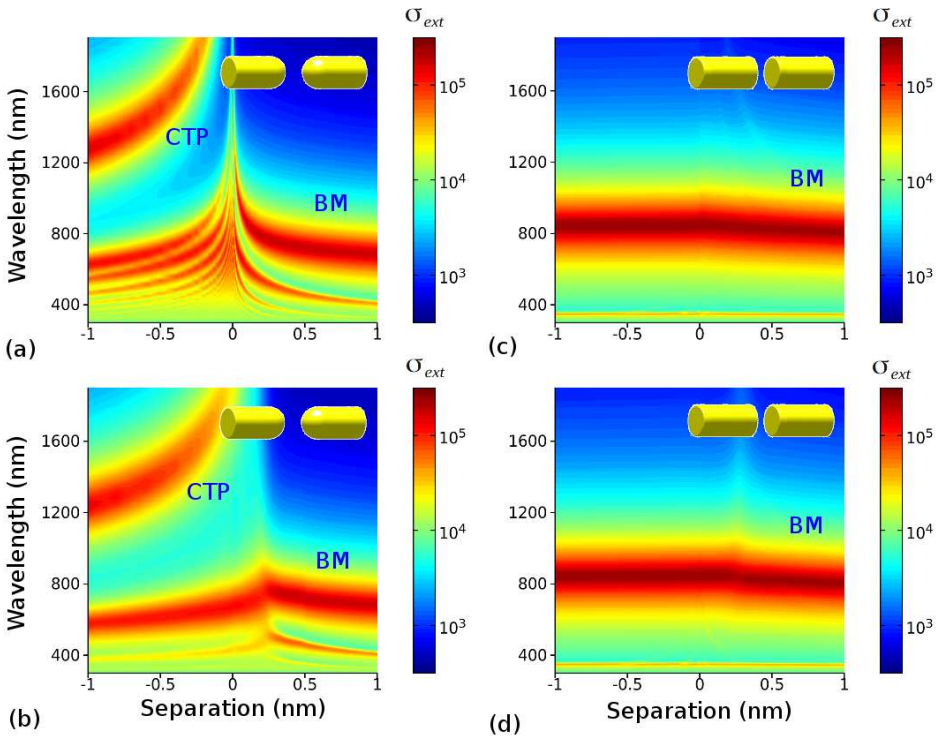

Figure 4. Extinction cross section of gap antennas. Classical simulations for (a) spherical-gap antennas and (b) for flat-gap antennas. QCM simulations for (c) spherical-gap antennas and (d) for flat-gap antennas. We indicate in the figures the nature of some of the modes (BMs and CTPs).

The classical calculations for the spherical-gap antenna [Figures 4(a) and 5(a)] at very short distances emphasize how the BMs redshift very strongly and the fields diverge as the gap distance approaches contact, where an unphysical discontinuity is formed. The BMs found in the extinction spectra [Figure 4(a)] are also identified by the strong near-field enhancement that diverges as the gap distance approaches zero [Figure 5(a)]. After contact and with increasing overlapping, low energy charge transfer plasmons (CTPs) are clearly visible in the extinction cross section [Figure 4(a)]. The CTPs are plasmon resonances that redistribute the charge density along both arms of the antenna due to the possibility of electron transfer across the physical contact between the rods, so that each antenna arm may have a net charge. In particular, the lowest order CTP appears for a characteristical low energy and many higher order modes appear for larger energies. This response is very similar to the results of spherical dimers.[5]*

In contrast, classical calculations of the extinction cross section of flat-gap antennas [Figure 4(c)] present the saturation in the spectral position of the modes as the gap distance is reduced. This saturation is due to the capacitive nature of the gap, as mentioned in section 2. Once contact is established, a continuous rod is formed and therefore the modes behave as those of a $2L$ rod blueshifting slowly as the length is

* The classical simulations of Figures 4 and 5 where made by Dr. Ruben Esteban at DIPC

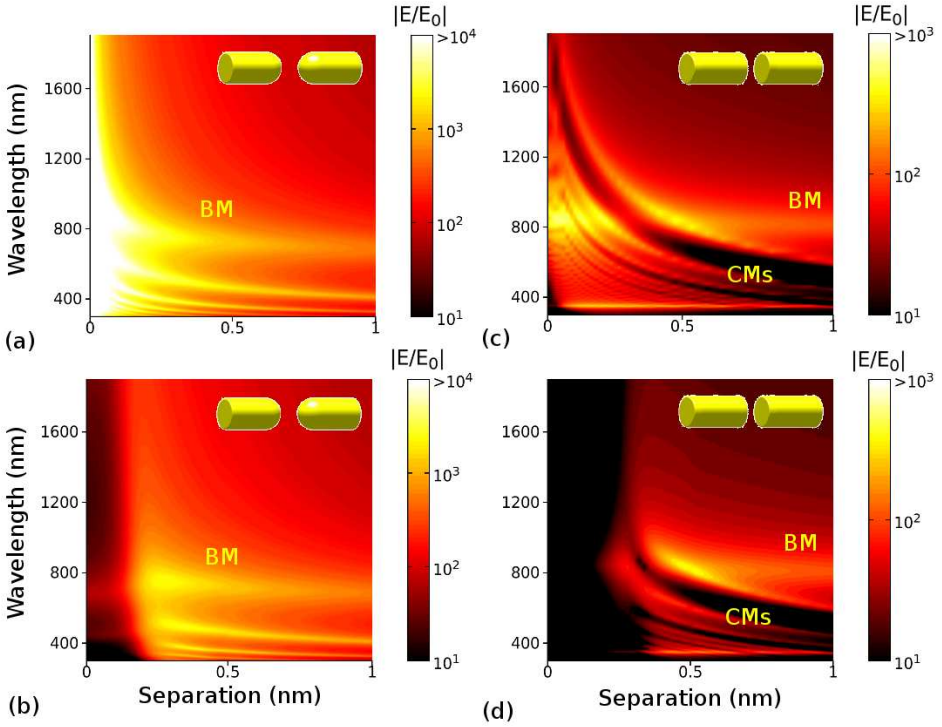

Figure 5. Near-field enhancement at gap-nanoantennas. Classical simulations for (a) spherical-gap antennas and (b) for flat-gap antennas. QCM simulations for (c) spherical-gap antennas and (d) for flat-gap antennas. We indicate in the figures the nature of some of the modes (BMs and CMs).

reduced[2] (not shown).

For the near-fields of the flat-gap antenna, the region of small separation distances shown in Figure 5(c) allows us to distinguish clearly the presence of the two sets of modes: a bonding mode (BM) at 800 nm which does not change with gap distance, and a set of cavity modes (CMs) that redshift strongly. It can be clearly observed how the cavity modes are very narrow in comparison with the far-field modes and they present a very strong redshift of their spectral position as the gap is reduced. Furthermore, Figure 5(c) also shows that the largest enhancements are produced for wavelengths and gap distances where cavity plasmon modes spectrally overlap with the bonding mode [yellow regions in Figure 5(c)].

We have thus shown that small gaps are very interesting from a fundamental point of view, as they reveal the cavity modes of flat terminations that are not present for spherical gaps. From a practical perspective, short distances are particularly interesting to produce strong field enhancements of practical use in field-enhanced spectroscopy. However, as pointed out, classical simulations do not account for quantum tunneling effects that become important for very narrow gaps. These effects should be included in a rigorous study of realistic systems. To do so we use the QCM described above. The QCM calculations of the extinction cross section for the spherical-gap antenna [Figure 4(b)] present a smooth transition between the non-touching and the overlapping regime.

They also show a change in the spectral position of the modes from red-shifting to blue-shifting at distances of approximately $0.2 - 0.3$ nm. Notably, the low energy CTP is already present even for positive distances, before physical contact, because quantum tunneling results in charge transfer across the gap, as if a conductive material was present. The CTPs blueshift as overlapping increases and they are fewer than for the classical case, because the tunneling softens the sharp edge region in the contact zone between the arms. The near-field enhancement of the spherical-gap antenna [Figure 5(b)] presents the same set of modes as the far-field spectrum [Figure 4(b)] but, at gap distances of approximately $0.2 - 0.3$ nm, a strong quenching of the modes is found. The pile-up of charges at the gap surfaces is responsible for the large enhancement of the near-field, thus, when charges are able to tunnel across the gap, the charge density gets screened and the near-fields are quenched.[10]

However, in the case of the flat-gap antenna [Figure 4(d)] we find that the tunneling hardly affects the far field because the gap behaves classically as a short-circuit, so that the additional conductivity has negligible effect in the spectrum in this case. In the near-field [5(d)], flat-end antennas show a quenching of the near-field, similar to the one in spherical gaps, but in this case the cavity modes are quenched at larger distances (~ 0.4 nm).

5. Conclusions

The morphology of the gap produces important modifications in the optical response of plasmonic gap-antennas, specially for small gap separation distances. Tunneling of charges across the gap affects differently the optical response depending on the geometry of the gap, as derived from our results for flat-gap and spherical-gap antennas.

We have shown that the consideration of tunneling between the antenna arms corrects the divergence of the local fields and the discontinuity found in the extinction cross section for spherical-gaps [Figures 5(b) and 4(b)]. Our model also provides a more physical connection between the high order modes found in the non-touching regime and the CTPs found in the overlapping regime. We have also observed how flat-gaps show plasmon cavity modes in the near-field that are not present in the the far-field [Figures 5(d) and 4(d)]. However, spherical-gaps present the same set of modes both, in the far-field and near-field spectra [Figures 5(b) and 4(b)]. Finally we have shown how tunneling produces the quenching of the near-fields when the gap distance is sufficiently small and that the particular details of this quenching also depends on the gap morphology [Figures 5(b) and 5(d)].

The results obtained here are important to design properly the morphology of gap antennas that can be used in field-enhanced spectroscopy and microscopy. As experimental situations reach subnanometric distances, quantum effects become relevant and need to be considered in any optical engineering approach.

Acknowledgments

I would like to thank Dr. Javier Aizpurua for giving me the opportunity to join his group to do the Master's Thesis with them. Special thanks to Dr. Ruben Esteban for his guidance and patience during all my learning process. Financial support from the Center for Materials Physics CSIC-UPV/EHU through a predoctoral grant of the Basque Excellence Research Center (BERC-MPC) is strongly acknowledged.

References

[1] Mühlschlegel P., Eisler H.-J., Martin O. J. F., Hecht B., Pohl D. W., *Science* **308,** 1607 (2005)
[2] Pelton M., Aizpurua J. and Bryant G., *Laser & Photonics Rev.* **2,** 136 (2008)
[3] Prodan E., Radloff C., Halas N. J., and Nordlander P., *Science* **302,** 419 (2003)
[4] Nordlander P., Oubre C., Prodan E., Li K. and Stockman M. I., *Nano Lett.* **4,** 899 (2004)
[5] Romero I., Aizpurua J., Bryant G.W and García de Abajo F.J., *Opt. Express* **14,** 9988 (2006)
[6] Vogelgesang R., Dmitriev A., *Analyst* **135,** 1175 (2010)
[7] Zuloaga J., Prodan E., and Nordlander P., *Nano Lett.* **9,** 887 (2009)
[8] Teperik T. V., Nordlander P., Aizpurua J., and Borisov A. G. *Phys. Rev. Lett.* **110,** 263901 (2013)
[9] Tame M. S., McEnery K. R., Özdemir Ş. K., Lee J., Maier S. A., and Kim M. S., *Nature Phys.* **9,** 329 (2013)
[10] Esteban R., Borisov A.G., Norlander P. and Aizpurua J., *Nature Commun.* **3,** 825 (2012)
[11] Alù A., and Engheta N., *Phys. Rev. Lett.* **101,** 043901 (2008)
[12] Novotny L., *Phys. Rev. Lett.* **98,** 266802 (2007)
[13] Joshi B. P., and Wei Q.-H., *Opt. Express* **16,** 10315 (2008)
[14] Bozhevolnyi S. I. and Søndergaard T., *Opt. Express* **15,** 10869 (2007)
[15] Savage K.J., Hawkeye M.M., Esteban R., Borisov A.G., Aizpurua J. and Baumberg J.J., *Nature* **491,** 574 (2012)